





Vertical distribution and longitudinal dispersion of gyrotactic microorganisms in a horizontal plane Poiseuille flow

Bohan Wang ^{1,*}, Weiquan Jiang ^{1,2,*}, Guoqian Chen ^{1,†}, Luoyi Tao ³ and Zhi Li¹

¹Laboratory of Systems Ecology and Sustainability Science, College of Engineering, Peking University, Beijing 100871, China

²State Key Laboratory of Hydrosience and Engineering, Department of Hydraulic Engineering, Tsinghua University, Beijing 100084, China

³Department of Aerospace Engineering, Indian Institute of Technology Madras, Chennai 60036, India



(Received 21 September 2020; accepted 16 April 2021; published 5 May 2021)

Dispersion of active Brownian particles is a fundamental issue in biological, environmental, and related applications. However, due to the restriction in former models, a detailed analysis of Taylor dispersion of gyrotactic microorganisms in a horizontal plane Poiseuille flow is still lacking. In the present paper, with a recently proposed method [Jiang and Chen, *J. Fluid Mech.* **877**, 1 (2019)], we illustrate the influences of the swimming ability, gyrotaxis intensity, shape anisotropy of microorganisms, and velocity of the ambient fluid on the dispersion process. Compared with nongyrotactic ones, there is a double accumulation mechanism for gyrotactic microorganisms: gravitactic focusing and wall accumulation. By using different boundary conditions, we show the effects of gravitactic focusing alone and double accumulation together. The variations of vertical distribution, overall drift, and effective dispersivity are characterized by changing the characteristic parameters of the microorganisms and the flow. Consisting of a swimming-induced part and an advection-induced part, the overall drift and effective dispersivity are coupled with the shape factor, flow Péclet number, and swimming Péclet number, which leads to nonmonotonic variations as functions of these parameters.

DOI: [10.1103/PhysRevFluids.6.054502](https://doi.org/10.1103/PhysRevFluids.6.054502)

I. INTRODUCTION

Much importance is attached to the transport of microorganisms in different environments, including confined channels [1,2], tubes [3,4], and porous media [5], which can be viewed as simplifications of practical environments such as bioreactors, rivers, blood vessels, and wetlands. Unlike solute, silt, and other passive matter, many kinds of microorganisms are motile and exhibit complicated dynamics, such as spontaneous accumulation at walls [6,7] and near-center depletion in pressure-driven channel flows [8]. Microorganisms do not swim meaninglessly and phenomena like algal blooms indicate that their collective motion is to strive for nutrients [9], lights [10], and other resources. For example, many kinds of phytoplankton swim upwards on average in quiescent water [11,12], enabling them to photosynthesize. This antigravity swimming behavior is called gravitaxis [13], which can be caused by the offset from the center of mass to the center of buoyancy of the microorganism cell [3]. In shear flows, the combined effect of the gravitational torque and the viscous torque, which is called gyrotaxis [13], will lead to some special phenomena such as gyrotactic focusing [3,14,15] and gyrotactic trapping [1,16].

*These authors contributed equally to this work.

†gqchen@pku.edu.cn

A single gyrotactic microorganism swims neither randomly exactly like a Brownian particle nor in a specified direction. Instead, its motion can be characterized as a biased random walk [17], which is an extension of Brownian motion. Though a microorganism is too big to observe conventional rules for Brownian motion, we can generalize the unbiased random walks theory with consideration of other influential factors. The most direct effects of the environment on gyrotactic microorganisms are the gravitational torque (related to the gyrotaxis intensity) and the viscous torque (related to the shape of the cells) [18], which are characterized by two dimensionless parameters named the bias parameter and the shape factor.

It is feasible and straightforward to model the motion of microorganisms with individual-level simulations [7,19,20], but it is also important to find out their macrotransport behaviors such as distribution, drift, and dispersivity via continuum-based methods. Taylor-Aris dispersion theory [21–23] has served researches of macrotransport process for many years. Effective methods have been well established to study the dispersion of passive particles [21–25], and efforts have also been made to extend these analytical methods to active dispersion [2,4,17,26]. The difficulty is that the governing equation of the microtransport process is a six-dimensional advection-diffusion equation covering both the positional and orientational fluxes. To simplify this rather complex equation to a conventional three-dimensional advection-diffusion equation in the position space, two parameters should be determined, named the mean swim direction vector and dispersivity tensor. For nongyrotactic active particles, after applying a small wave-number expansion to the Smoluchowski equation, Peng and Brady [27] recently analyzed the dispersion in a Poiseuille flow using orientational moment expansion and finite element method. For gyrotactic microorganisms, the transport problem is more complex due to the gyrotactic term. The Pedley-Kessler (PK) model [28] is a pioneering work and has been used in determining these two coefficients in many works [4,13,29–32]. A Fokker-Planck equation for the orientational probability is employed to calculate the drift vector and the dispersivity tensor in the PK model. However, the PK model is only valid for weak shear flows, low swimming speed, and weak confinement situations [2,33]. Apart from the PK model, the generalized Taylor dispersion (GTD) theory was also applied to dispersion of gyrotactic microorganisms in unbounded homogeneous shear flows [25]. Bearon *et al.* [17] attempted to extend the GTD model to inhomogeneous shear flows by using an imaginary unbounded homogeneous shear flow to substitute the local flow, but the accuracy of GTD results was still limited when the shear variation is large and when the boundary effects are not negligible, as can be seen by comparing with the individual-based simulations in their work.

Although the PK model and traditional GTD method are obligatory to study the transport process of gyrotactic microorganisms in three dimensions, the dispersion in confined flows can be analytically derived by a one-step generalized Taylor dispersion theory recently put forward by Jiang and Chen [34]. GTD theory indicates that, in the long-time asymptotic state, the zeroth-order moment of microorganism probability density (integrating over the unbounded coordinate) satisfies a no-flux equation in the local space [35]. In other words, by setting the unbounded streamwise coordinate as the only global coordinate, GTD theory can be directly applied to derive the dispersion process in the streamwise direction without restrictions that the former methods suffer. As a consequence, the one-step GTD method is accurate for investigating the dispersion process in confined flows. Soon after the one-step method was proposed, Jiang and Chen [36] studied the gyrotactic focusing phenomenon and its influence on the dispersion in a vertical Poiseuille flow. However, they did not consider the dispersion of gyrotactic microorganisms in a horizontal flow, which exists widely in natural and artificial environments. Also, the dispersion in a horizontal flow is fundamentally different: the gravitaxis will drive microorganisms to accumulate near the upper boundary [37,38], which is called gravitactic focusing [17]. Gravitactic focusing may greatly affect the dispersion process, however it is not well understood yet due to former model restrictions.

Apart from the gravitactic focusing, there is another mechanism of near-boundary accumulation. For stationary suspension of active particles confined by solid walls, an interesting phenomenon is the wall accumulation which has been observed in the suspension of spermatozoa and *E. coli* [6,7]. The mechanism underlying wall accumulation is explored by researchers from different

perspectives. Far-field hydrodynamic interactions between cells and walls are extensively studied [7,19,39,40] and reproduce basic features of the wall accumulation phenomenon. However, in some numerical works incorporating the hydrodynamic effects, the wall accumulation is even more intensive in dilute suspensions [19,41], indicating a different perspective to understand this phenomenon. Considering direct flagellar contact dynamics alone, Li *et al.* [20,42] simulated the distribution of *E. coli* and *C. crescentus*, and found better agreement with the experiments than the hydrodynamic models. The view that steric interactions instead of hydrodynamic interactions play a more important role in cell-wall interactions is reinforced and developed by further studies [9,43–45].

We note that the above-mentioned descriptions of the boundary behaviors of microorganisms are majorly on the individual scale. From a continuum perspective, Elgeti and Gompper [44] used a set of zero-flux boundary conditions (Robin type) to solve their continuum-based model based on a Fokker-Planck equation. Their results confirmed that the Robin type boundary conditions can characterize the wall accumulation. Ezhilan and Saintillan [45] presented a detailed analysis of wall accumulation, upstream swimming, and centerline depletion of active particles with different shape anisotropy in a pressure-driven channel flow; their results again showed that the simple Robin type boundary conditions can capture the key features in the transport of dilute suspensions of microorganisms. Recently, Peng and Brady [27] investigated the upstream swimming and Taylor dispersion of active Brownian particles in a pressure-driven flow. They also used the Robin type boundary conditions in solving the continuum-based equation. The Robin type boundary conditions ensure that the total probability flux normal to the boundary is zero. Another set of boundary conditions that also satisfy the zero-total-flux condition is the reflective boundary conditions, which assumes the collisions between cells and boundaries are perfectly elastic. The reflective boundary conditions can be also implemented in solving continuum-based equations [46,47] and in doing Brownian dynamic simulations [2,8,17,48].

In the present paper, following the one-step method, we aim to investigate the active dispersion process under gravitactic focusing and wall accumulation in a horizontal plane Poiseuille flow. This double accumulation mechanism may greatly affect the Taylor dispersion process. To decouple the double accumulation, we first analyze the dispersion under gravitactic focusing alone by imposing the reflective boundary conditions. Then we analyze the dispersion under double accumulation by imposing the Robin type boundary conditions. Some scholars have studied the dispersion process of gyrotactic microorganisms [2,4,14,33,36,37], but their researches either focused on vertical flows or were based on the approximate methods (PK, GTD, or Stokes-dynamics based). The boundary effects in vertical flows are not as obvious as they are in horizontal flow [2,17], thus the approximate methods may hold. However, the dispersion of gyrotactic microorganisms in horizontal plane Poiseuille flow, which is severely affected by the boundary effects, deserves an in-depth investigation. Motivated by this, the shape factors, bias parameters, swimming ability of the microorganisms, and average flow velocity are set to be variable in this paper to give a detailed analysis of this process.

II. MATHEMATICAL FORMULATION

A. Governing equations

Although a microorganism is too large to be considered as a conventional Brownian particle, the analogy has been made between the motion of microorganisms and the Brownian motion [28] that contains translational diffusion and rotational diffusion. Under the assumption that the suspension of microorganisms is dilute enough for negligible cell-cell and cell-fluid interactions (one-way coupling), the Smoluchowski equation [49] of the probability density function (PDF) P in the position-orientation space $(\mathbf{R}^*, \mathbf{p})$ is adopted as

$$\frac{\partial P}{\partial t^*} + \nabla_R^* \cdot \mathbf{J}_R^* + \nabla_p \cdot \mathbf{J}_p^* = 0, \quad (1)$$

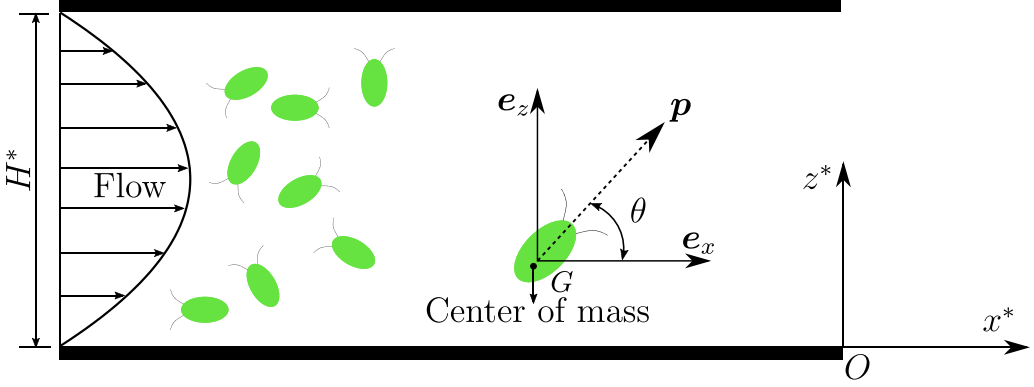


FIG. 1. Sketch of gyrotactic microorganisms in a horizontal plane Poiseuille flow.

where P is the probability of a microorganism found in the position vector \mathbf{R}^* with the orientation vector \mathbf{p} at time t^* . $\nabla_{\mathbf{R}}^*$ and $\nabla_{\mathbf{p}}$ denote the gradient operators in the position and orientation space, respectively;

$$\mathbf{J}_{\mathbf{R}}^* = [\mathbf{U}^*(\mathbf{R}^*) + V_s^* \mathbf{p}]P - D_t^* \nabla_{\mathbf{R}}^* P \quad (2)$$

is the probability flux in the position space, and

$$\mathbf{j}_{\mathbf{p}}^* = \dot{\mathbf{p}}^* P - D_r^* \nabla_{\mathbf{p}} P \quad (3)$$

is the probability flux in the orientation space. \mathbf{U}^* is the velocity of the ambient flow. V_s^* is the average swimming speed of the microorganisms, which is a constant scalar. D_t^* and D_r^* are the intrinsic translational and rotational diffusivity coefficients similar to those of Brownian particles, which represent the random part of the motion.

Microorganisms change their directions at a rate

$$\dot{\mathbf{p}}^* = \boldsymbol{\Omega}_a^* \times \mathbf{p}, \quad (4)$$

where a dot above denotes the derivative of time. $\boldsymbol{\Omega}_a^*$ is the total angular velocity of the microorganisms [13], which is calculated by

$$\boldsymbol{\Omega}_a^* = -\frac{1}{2B^*} \mathbf{p} \times \mathbf{k} + \frac{1}{2} \boldsymbol{\omega}^* + \alpha_0 [\mathbf{p} \times (\mathbf{E}^* \cdot \mathbf{p})], \quad (5)$$

where B^* is the gyrotactic orientation parameter [50] equaling to the reorientation time of direction vector \mathbf{p} under the balance of constant gravity offset torque and viscous torque. \mathbf{k} is the unit vector opposing the gravity;

$$\boldsymbol{\omega}^* = \nabla_{\mathbf{R}}^* \times \mathbf{U}^* \quad (6)$$

is the vorticity of the ambient flow, and

$$\mathbf{E}^* = \frac{1}{2} [\nabla_{\mathbf{R}}^* \mathbf{U}^* + (\nabla_{\mathbf{R}}^* \mathbf{U}^*)^T] \quad (7)$$

is the strain-rate tensor. The microorganism is considered an ellipsoid with a shape factor α_0 reflecting the anisotropy (Bretherton constant [51]). α_0 ranges from 0 (sphere) to 1 (infinitely thin rod).

B. Dimensionless formulation

In a horizontal plane Poiseuille flow with height H^* , as shown in Fig. 1, position coordinates x^* and z^* with unit vector \mathbf{e}_x and \mathbf{e}_z and orientation coordinates ρ and θ with unit vector \mathbf{p} and \mathbf{e}_θ are

used for the position and orientation space, respectively; then

$$\mathbf{U}^* = U^*(z^*)\mathbf{e}_x, \quad (8)$$

where U^* is the speed of the ambient flow, and

$$\mathbf{p} = \mathbf{e}_\rho = p_x(\theta)\mathbf{e}_x + p_z(\theta)\mathbf{e}_z \quad (9)$$

is the swimming direction, where

$$p_x = \cos \theta, \quad p_z = \sin \theta, \quad (10)$$

where θ is the angle between \mathbf{p} and \mathbf{e}_x .

Dimensionless variables and parameters are defined by

$$\begin{aligned} t &= t^*D_r^*, & x &= \frac{x^*}{H^*} - \text{Pe}_f t, & z &= \frac{z^*}{H^*}, & U &= \frac{U^*}{U_m^*} - 1, \\ \text{Pe}_s &= \frac{V_s^*}{D_r^*H^*}, & \text{Pe}_f &= \frac{U_m^*}{D_r^*H^*}, & D_t &= \frac{D_t^*}{D_r^*H^{*2}}, & \lambda &= \frac{1}{2B^*D_r^*}, \end{aligned} \quad (11)$$

where U_m^* is the depth average velocity calculated by

$$U_m^* \triangleq \frac{1}{H^*} \int_0^{H^*} U^*(z^*) dz^*. \quad (12)$$

Pe_s is the swimming Péclet number for the ratio between swimming speed and rotational diffusion, Pe_f is the Péclet number for the ratio between the depth average flow velocity and rotational diffusion, D_t is the ratio of translational diffusivity to the rotational diffusivity, and λ is the dimensionless bias parameter.

The dimensionless form of the probability conservation equation (1) becomes

$$\frac{\partial P}{\partial t} + \nabla_R \cdot [(\text{Pe}_f U \mathbf{e}_x + \text{Pe}_s \mathbf{p})P - D_t \nabla_R P] + \nabla_p \cdot (\dot{\mathbf{p}}P - \nabla_p P) = 0, \quad (13)$$

where $\nabla_R = \mathbf{e}_x \frac{\partial}{\partial x} + \mathbf{e}_z \frac{\partial}{\partial z}$, $\nabla_p = \mathbf{e}_\theta \frac{\partial}{\partial \theta}$, and

$$\dot{\mathbf{p}} = \dot{\theta} \mathbf{e}_\theta, \quad (14)$$

where

$$\dot{\theta} = \frac{1}{2} \text{Pe}_f \frac{\partial U}{\partial z} (-1 + \alpha_0 \cos 2\theta) + \lambda \cos \theta. \quad (15)$$

C. Boundary conditions and the initial condition

Conservation of particles requires zero-total-flux condition at the boundaries. The zero-total-flux condition is specified as

$$\int_0^{2\pi} \mathbf{e}_z \cdot \mathbf{J}_R d\theta = \int_0^{2\pi} \left(\text{Pe}_s \sin \theta P - D_t \frac{\partial P}{\partial z} \right) d\theta = 0 \quad \text{at } z = 0, 1. \quad (16)$$

Elgeti and Gompper [44] used a set of Robin type boundary conditions

$$\text{Pe}_s \sin \theta P - D_t \frac{\partial P}{\partial z} = 0 \quad \text{at } z = 0, 1, \quad (17)$$

which satisfies the zero-total-flux condition (16) and illustrates the balance between swimming flux and translational diffusion flux in the boundary-normal direction. We note that $D_t = 0$ induces singularity under the Robin boundary conditions, as pointed out by Ezhilan and Saintillan [45] and studied by Peng and Brady [27] using Brownian dynamics simulations. This singular limit will not be discussed in this paper and we set D_t to be a positive constant under the Robin boundary conditions.

The reflective boundary conditions [17,34,36] also satisfy the zero-total-flux condition (16):

$$P(x, z, \theta, t) = P(x, z, -\theta, t) \quad \text{at } z = 0, 1, \quad (18)$$

$$\frac{\partial P}{\partial z}(x, z, \theta, t) = -\frac{\partial P}{\partial z}(x, z, -\theta, t) \quad \text{at } z = 0, 1. \quad (19)$$

However, this set of boundary conditions is unable to capture the wall accumulation [34,45].

Periodic conditions for θ are

$$\begin{aligned} P|_{\theta=0} &= P|_{\theta=2\pi}, \\ \frac{\partial P}{\partial \theta}|_{\theta=0} &= \frac{\partial P}{\partial \theta}|_{\theta=2\pi}. \end{aligned} \quad (20)$$

The initial condition for P is formally given as

$$P|_{t=0} = P^{(0)}(x, z, \theta), \quad (21)$$

which according to the GTD theory [35] does not influence the long-time solution for the dispersion process as long as the initial patch is released in a compact range. As we are concerned about the steady state dispersion, a specific initial condition is not required.

III. SOLUTIONS FOR THE GENERALIZED TAYLOR DISPERSION MODEL

A. Local and global space

As a channel is mostly associated with a longitudinal length scale much greater than its transverse scale, the longitudinal dispersion process is of great interest. According to the one-step GTD method [34], the global space \mathcal{Q} and local space \mathbf{q} are chosen as

$$\mathcal{Q} \triangleq \{x\}, \quad \mathbf{q} \triangleq \{z, \theta\}. \quad (22)$$

The conservation equation (13) can be recast as

$$\frac{\partial P}{\partial t} + [\text{Pe}_s \cos \theta + \text{Pe}_f U(z)] \frac{\partial P}{\partial x} - D_t \frac{\partial^2 P}{\partial x^2} + \mathcal{L}P = 0, \quad (23)$$

where \mathcal{L} is an operator in local space \mathbf{q} defined as

$$\mathcal{L}P \triangleq \text{Pe}_s \sin \theta \frac{\partial P}{\partial z} - D_t \frac{\partial^2 P}{\partial z^2} + \frac{\partial(\dot{\theta}P)}{\partial \theta} - \frac{\partial^2 P}{\partial \theta^2}.$$

The integration of P over the local space is denoted as

$$\langle P \rangle \triangleq \int_0^1 dz \int_0^{2\pi} d\theta P(x, z, \theta, t), \quad (24)$$

which represents the mean concentration of microorganisms in the longitudinal direction \mathbf{e}_x .

B. Zeroth-order longitudinal moment

The long-time asymptotic state of the zeroth-order longitudinal moment of P is

$$P_0^\infty(z, \theta) \triangleq \lim_{t \rightarrow \infty} \left(\int_{-\infty}^{+\infty} P(x, z, \theta, t) dx \right), \quad (25)$$

which is the steady local distribution in the local space \mathbf{q} . The boundary conditions for P_0^∞ are the same as those for P . According to the GTD theory, P_0^∞ satisfies

$$\mathcal{L}P_0^\infty = 0, \quad (26)$$

which can be solved by a Galerkin method with basis functions satisfying the reflective boundary conditions.

In basis functions construction, variables separation is more complicated under the Robin type boundary conditions. Following Jiang and Chen [34], we decompose P_0^∞ into

$$P_0^\infty = P_a G_0, \quad (27)$$

where

$$P_a = \exp\left[\frac{\text{Pe}_s \sin\theta(z - \frac{1}{2})}{D_t}\right]. \quad (28)$$

The boundary conditions for G_0 can be obtained by substituting Eq. (27) into Eq. (17):

$$\frac{\partial G_0}{\partial z} = 0 \quad \text{at } z = 0, 1. \quad (29)$$

Equation (26) becomes

$$\mathcal{L}_0 G_0 = 0, \quad (30)$$

where $\mathcal{L}_0(\cdot) \triangleq \frac{1}{P_a} \mathcal{L}(P_a(\cdot))$. G_0 and its first derivative with respect to θ also satisfy the periodic condition

$$\begin{aligned} G_0|_{\theta=0} &= G_0|_{\theta=2\pi}, \\ \frac{\partial G_0}{\partial \theta} \Big|_{\theta=0} &= \frac{\partial G_0}{\partial \theta} \Big|_{\theta=2\pi}. \end{aligned} \quad (31)$$

G_0 can be also solved with basis functions satisfying the Robin boundary conditions (29).

C. Overall drift and dispersivity

As basic phenomenological macrotransport properties of a dispersion process, the overall drift velocity U_d and the Taylor dispersivity coefficient D_T are important to understand the process. The long-time solutions for U_d and D_T in the longitudinal direction describe the drift velocity above the mean flow and the effective diffusivity. U_d and D_T can be defined as [35]

$$U_d \triangleq \lim_{t \rightarrow \infty} \frac{dM_1}{dt}, \quad (32)$$

$$D_T \triangleq \frac{1}{2} \lim_{t \rightarrow \infty} \frac{d}{dt} (M_2 - M_1^2), \quad (33)$$

where M_i is the i th moment of $\langle P \rangle$:

$$M_i \triangleq \int_{-\infty}^{\infty} x^i \langle P \rangle dx \quad i = 0, 1, 2, \dots \quad (34)$$

Generalized Taylor dispersion theory indicates that U_d and D_T are subject to

$$U_d = \langle P_0^\infty V_x \rangle, \quad (35)$$

$$D_T = D_t + \langle b V_x \rangle, \quad (36)$$

where V_x is the overall longitudinal speed of microorganisms:

$$V_x(z, \theta) = \text{Pe}_f U + \text{Pe}_s \cos \theta; \quad (37)$$

b is a function independent of time to be determined and satisfies

$$\mathcal{L}b(z, \theta) = P_0^\infty (V_x - U_d), \quad (38)$$

$$\langle b(z, \theta) \rangle = 0. \quad (39)$$

For the reflective boundary conditions, the boundary conditions and periodic conditions for b are the same as those for P [Eqs. (18)–(20)]. For the Robin boundary condition, b is also decomposed in the same way as P_0^∞ :

$$b = P_a G_b, \quad (40)$$

where G_b satisfies

$$\mathcal{L}_0 G_b(z, \theta) = G_0 (V_x - U_d). \quad (41)$$

The boundary conditions and periodic condition for G_b are the same as those for G_0 stated in Eqs. (29) and (31). b (for reflective boundary conditions) and G_b (for Robin boundary conditions) can be solved with similar procedures to solving P_0^∞ and G_0 , respectively, and the results are expressed by a series of the basis functions.

IV. RESULTS AND DISCUSSION

The dimensionless velocity profile of the horizontal plane Poiseuille flow is

$$U(z) = 6z(1 - z) - 1. \quad (42)$$

A. Vertical distribution

The vertical distribution of the microorganisms is calculated by

$$\langle P_0^\infty \rangle_O = \int_0^{2\pi} P_0^\infty(z, \theta) d\theta. \quad (43)$$

We note that vertical distribution of gyrotactic microorganisms in a horizontal plane Poiseuille flow has been investigated by several researchers [37,38]. For example, with the local mean swimming orientation and diffusion tensor obtained from Stokes dynamics of interacting cells, Ishikawa [37] examined the evolution of the vertical distribution of an initially uniformly distributed cell patch. However, due to the employed local equilibrium hypothesis, the concentration at the upper wall became unrealistically high and the steady state could not be accurately obtained.

Bearon *et al.* [17] indicated an exponential distribution for spherical gyrotactic microorganisms in horizontal unidirectional flows by analyzing the effective vertical transport equation. In the current notion, the distribution can be written as

$$P_0^\infty(z, \theta) = \frac{\lambda}{2\pi \text{Pe}_s (e^{\lambda/\text{Pe}_s} - 1)} e^{\frac{\lambda z}{\text{Pe}_s}}. \quad (44)$$

We note that the exponential distribution is unrelated to the swimming direction of the microorganisms, therefore it satisfies the reflective boundary conditions of probability (18). However, the exponential distribution is only valid for cases when the translational diffusivity is neglected, i.e., $D_t = 0$. As shown in Fig. 2, the exponential distribution (44) is close to the results under the reflective boundary conditions in the current paper. But this distribution does not satisfy the reflective boundary conditions of probability gradient (19) which we impose to satisfy the zero-total-flux condition. Not only that, the probability gradient normal to the boundary is nonzero, i.e., it does not satisfy the zero-total-flux condition (16) if $D_t \neq 0$.

1. Influences of the bias parameter and swimming Péclet number

We first discuss the spherical swimmers ($\alpha_0 = 0$), which resemble most algae. The bias parameter λ reflects the strength of gravitaxis, which drives the microorganisms to swim upwards, for example, $\lambda \approx 2$ for *C. nivalis* [52,53] and $\lambda \approx 1.79$ for *Volvox* [54] and *H. akashiwo* [55]. We take four different values for λ with the shape factor α_0 fixed at zero. Pe_s and Pe_f are nondimensionalized parameters involving the channel height, swimming velocity, flow velocity, and rotational diffusivity. For example, in a channel with depth $H^* = 1$ cm and mean velocity $U_m^* = 6.3 \times 10^{-3}$ m s⁻¹,

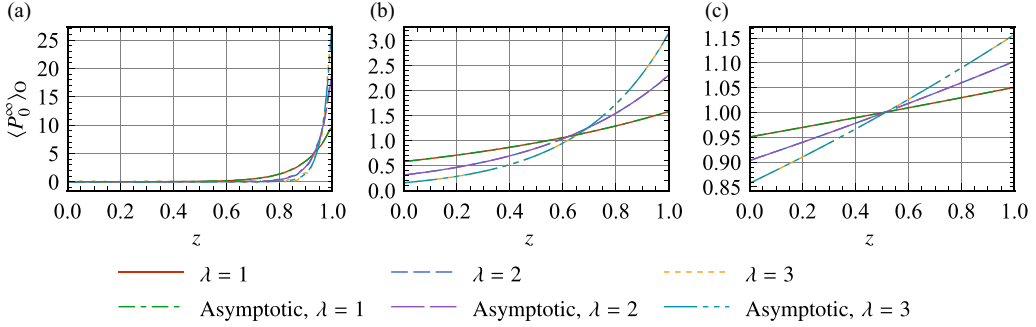


FIG. 2. Vertical distributions $\langle P_0^\infty \rangle_0$ of spherical microorganisms under the reflective boundary conditions with zero translational diffusivity ($D_t = 0$). Swimming Péclet numbers Pe_s at left, middle, and right are 0.1, 1, and 10, respectively. λ denotes the bias parameter of microorganisms. “Asymptotic” denotes the exponential distribution (44).

C. nivalis with $V_s^* = 6.3 \times 10^{-5} \text{ m s}^{-1}$ and $D_r^* = 0.067 \text{ s}^{-1}$ yields $Pe_s = 0.1$ and $Pe_f = 10$. We change Pe_s and Pe_f within several magnitudes in our analysis.

As shown in Fig. 3, in all cases, reflective boundary conditions do not lead to wall accumulation: the vertical distributions of spherical nongyrotactic swimmers ($\alpha_0 = 0, \lambda = 0$) are uniform, which can be predicted by their unbiased movement irrespective of strain and gyrotaxis as expected in Eq. (5). The dynamics of this kind of swimmers is similar to that of passive Brownian particles. With a nonzero bias parameter, microorganisms are gyrotactic and exhibit gravitactic focusing. The

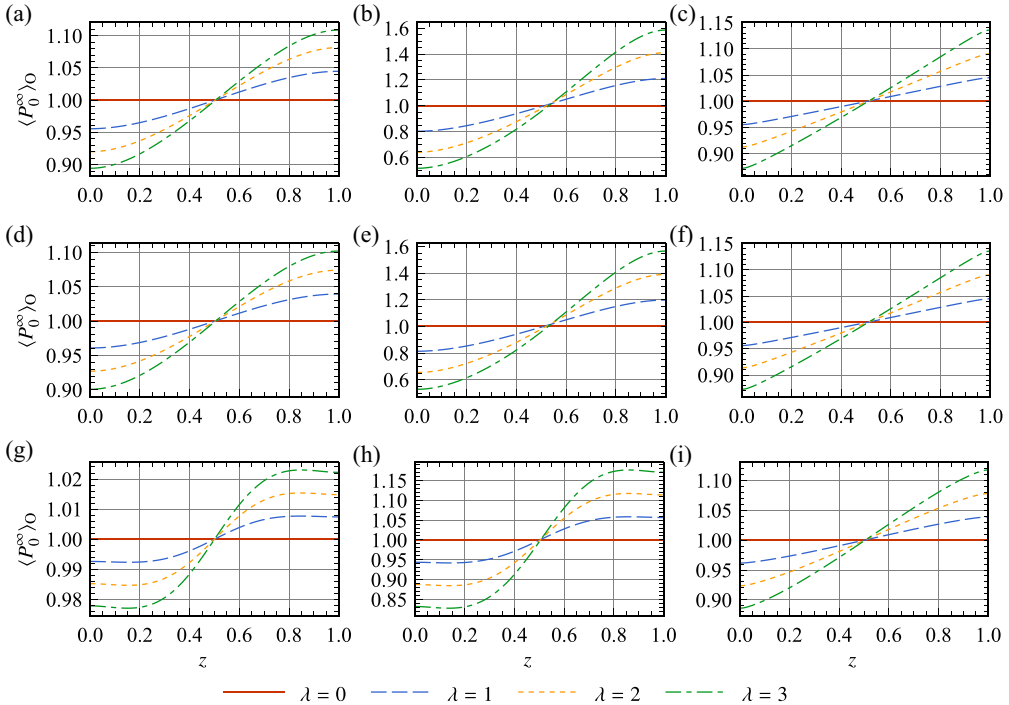


FIG. 3. Vertical distributions $\langle P_0^\infty \rangle_0$ of spherical microorganisms under the reflective boundary conditions. Swimming Péclet numbers Pe_s at left, middle, and right are 0.1, 1, and 10, respectively. Flow Péclet numbers Pe_f at top, middle, and bottom are 0.1, 1, and 10, respectively. $D_t = 1/6$ in all cases. λ denotes the bias parameter of microorganisms.

gravitactic focusing near the upper surface of microorganisms with larger λ is more obvious, as depicted in Figs. 2 and 3. As λ gets larger, the concentration near the water surface increases while the concentration in the bottom part and middle part decreases.

Another phenomenon that can be seen by comparing the subfigures in Figs. 2 and 3 is that, in the absence of translational diffusivity, gravitactic focusing near the water surface is weakened as Pe_s increases; however, with a constant translational diffusivity, gravitactic focusing shows nonmonotonic variation as a function of Pe_s . This can be understood by considering the idealized “stone skipping” behavior of microorganisms near the walls: when a microorganism swims upwards to the wall, it cannot pass through the wall, and due to the imposed reflective boundary conditions it will subsequently swim downwards to the bulk of the channel; after a while, it swims upwards again due to gyrotaxis. In the absence of translational diffusivity, if the swimming ability (quantified by Pe_s) is weak, microorganisms take a shorter distance to swim upwards again and the gyrotactic focusing is more intensive in the final steady state, as shown in Fig. 2. However, when a constant translational diffusivity is applied, the variation becomes nonmonotonic. As shown in Fig. 3, the gyrotactic focusing is most intensive at moderate swimming ability ($Pe_s = 1$). When the swimming ability is weak, the translational diffusion dominates over the gravitactic focusing induced by swimming; when the swimming ability is strong, the stone skipping also inhibits gravitactic focusing; only in a moderate range of swimming ability does gravitactic focusing reach its maximum. Additionally, the flow Péclet number Pe_f can affect the concentration profile near the upper wall. As depicted in Figs. 3(g) and 3(h), the concentration decreases as $z \rightarrow 1$. In these cases, gravitactic focusing is greatly inhibited by the strong near-wall shear.

2. Influence of the shape factor

In the discussion above, we only consider the vertical distribution of spherical microorganisms. Spherical microorganisms are only subject to the rotation of the ambient fluid while elongated microorganisms are also subject to the strain as expected in Eq. (5). To explore the influence of shape factor α_0 on the vertical distribution, we fix the bias parameter λ at 2 and change α_0 from 0 to 1. Nonzero α_0 is often related to bacteria such as *E. coli* and *C. crescentus*, but some algae are also anisotropic in shape, at least if their flagella are considered.

As shown in Fig. 4, when the flow Péclet number Pe_f is not too large (≤ 1), vertical distributions of all microorganisms with various shape factors are almost identical. However, in Figs. 4(g)–4(i), i.e., when Pe_f is large, the vertical distributions of microorganisms with different α_0 exhibit significant differences: the slenderer the microorganisms, the more obvious the accumulation at the upper wall. This can be attributed to the shear alignment effect, which can be intuitively understood by analyzing the orientational distribution of microorganisms. As shown in Fig. 5, in the orientation space, the concentration of microorganisms near $\theta = \pi$ and 0 (also $\theta = 2\pi$), becomes more intensive with larger α_0 . It can be readily understood by considering the Jeffery rotations under which the elongated microorganisms prefer to swim horizontally both upstream and downstream. Microorganisms with smaller α_0 suffer weaker strain effect and have a more uniform distribution in the orientation space. It should be noted that in Fig. 4(i) the concentration of highly elongated microorganisms near the bottom is also higher than that of spherical microorganisms. It can be explained by the fact that part of extremely slender ($\alpha_0 = 1$) and highly active ($Pe_s = 10$) microorganisms can easily reach and be also trapped near the bottom wall, where the local shear is as high as in the upper wall.

B. Drift and dispersivity

1. Influence of the swimming Péclet number

We now characterize the drift U_d and dispersivity D_T of gyrotactic microorganisms as a function of Pe_s . It can be clearly seen in Figs. 6 and 7 that the drift U_d shows nonmonotonic variation as a function of the swimming Péclet number Pe_s , namely, a transition between positive correlation and

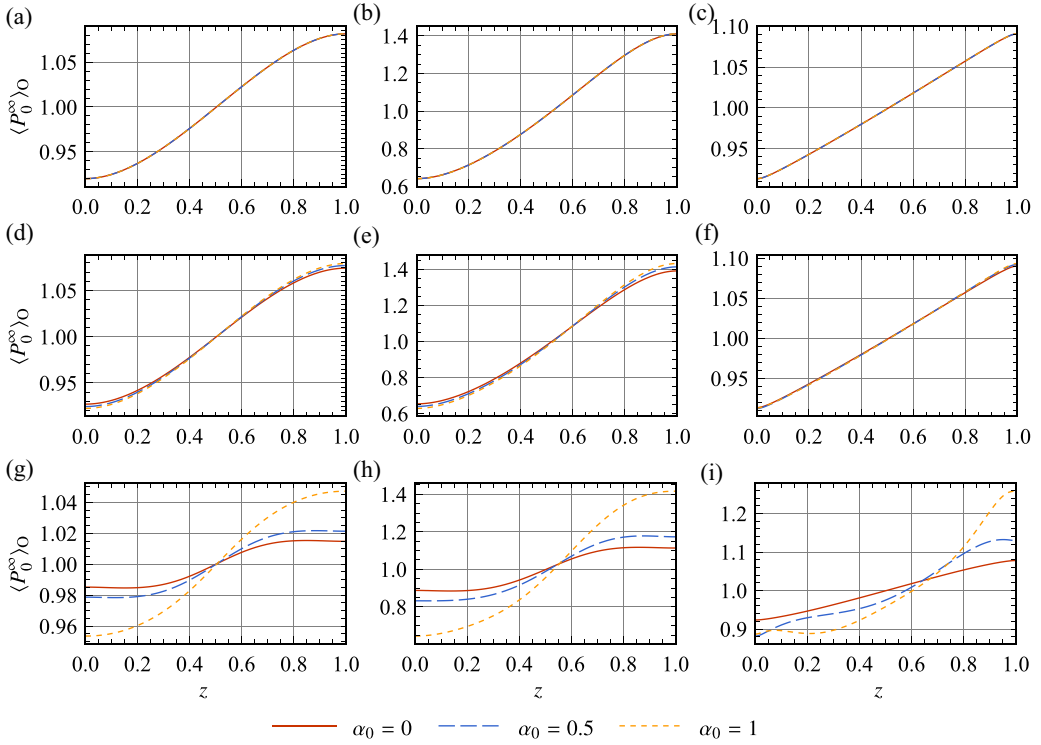


FIG. 4. Vertical distributions $\langle P_0^\infty \rangle_0$ of microorganisms under the reflective boundary conditions with fixed bias parameter $\lambda = 2$. Swimming Péclet numbers Pe_s at left, middle, and right are 0.1, 1, and 10, respectively. Flow Péclet numbers Pe_f at top, middle, and bottom are 0.1, 1, and 10, respectively. $D_t = 1/6$ in all cases. α_0 denotes the shape factor of microorganisms.

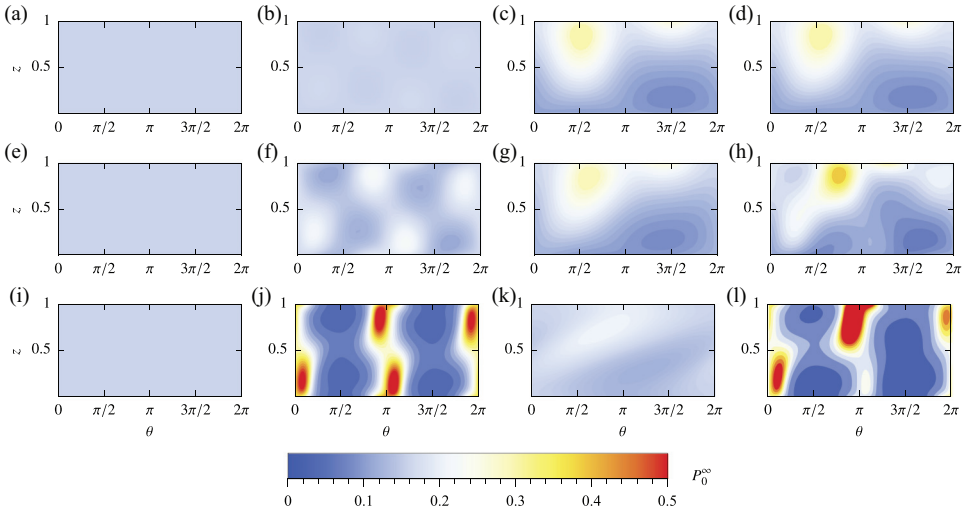


FIG. 5. $P_0^\infty(z, \theta)$ of microorganisms in the local space \mathbf{q} under the reflective boundary conditions. First row, $Pe_f = 0.1$; second row, $Pe_f = 1$; third row, $Pe_f = 10$. The left two columns are for nongyrotactic microorganisms and the right two columns are for gyrotactic microorganisms with $\lambda = 2$. $\alpha = 0$ in the first column and third column and $\alpha = 1$ in the second column and fourth column. $Pe_s = 1$, $D_t = 1/6$ in all cases.

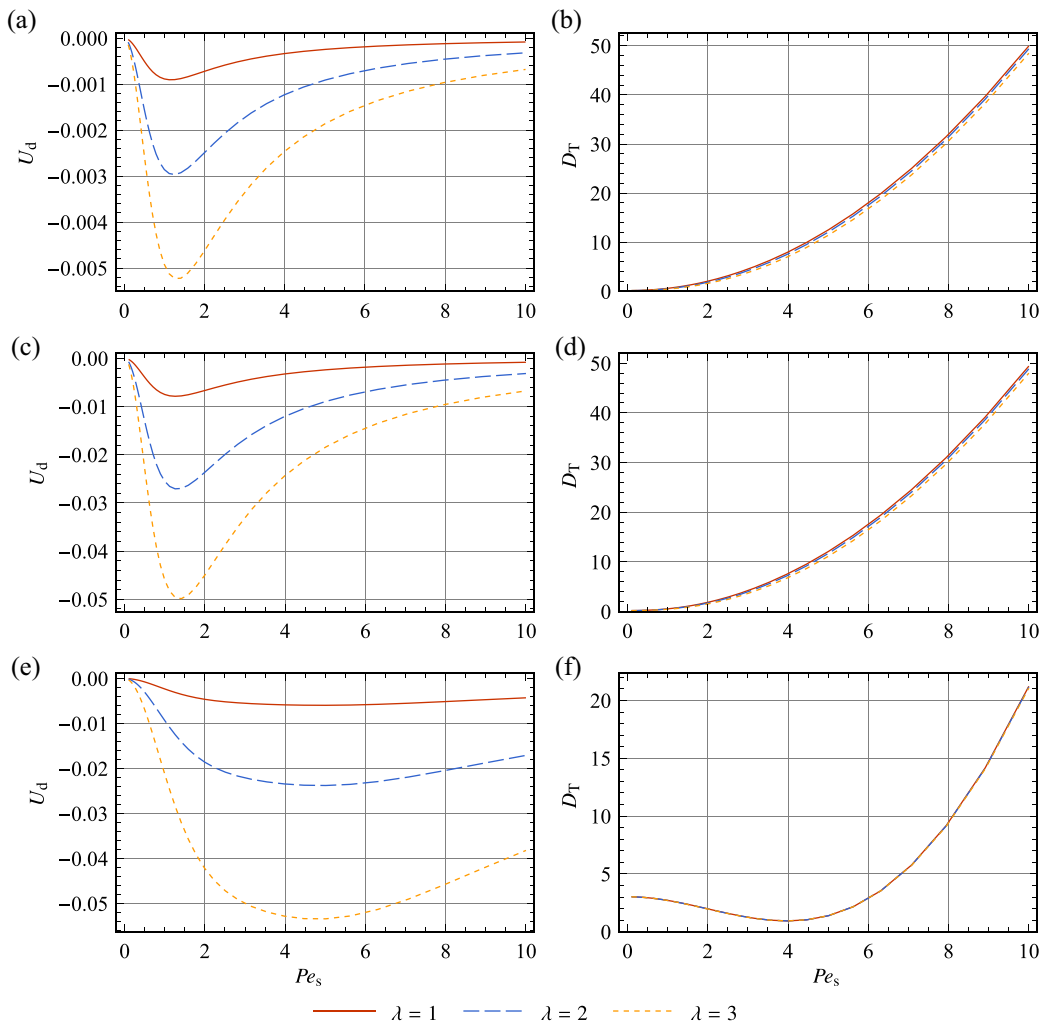


FIG. 6. Overall drift U_d and dispersivity D_T as functions of swimming Péclet number Pe_s under the reflective boundary conditions with fixed shape factor $\alpha_0 = 0$. Top, $Pe_f = 0.1$; middle, $Pe_f = 1$; bottom, $Pe_f = 10$. In all cases, $D_t = 1/6$.

negative correlation can be found. As clearly indicated in the definition (35), the drift U_d includes two parts: the advection part $\langle P_0^\infty Pe_f U \rangle$ and the swimming part $\langle P_0^\infty Pe_s \cos \theta \rangle$, both of which are determined by the local distribution P_0^∞ . For the advection part, it can be further simplified to $Pe_f \int_0^1 U \langle P_0^\infty \rangle_O dz$, which can be directly determined by the vertical distribution $\langle P_0^\infty \rangle_O$. As shown in Fig. 3, the gravitactic focusing is most intensive at a moderate Pe_s . Evidently, the intensive gravitactic focusing greatly enhances the drift due to the fast local advection speed. For the swimming part, because the microorganisms considered in Fig. 6 are spherical, their orientational distribution is not strongly polarized, as shown in Fig. 5. The nonpolarized orientational distribution has a negligible contribution to the overall drift U_d . Based on the discussion above, the nonmonotonic variation of U_d as a function of Pe_s can be understood. Also, we can expect that, as Pe_s continues increasing, U_d will tend to zero, which means a uniform vertical distribution and the center of the cells cloud moving along with the average flow.

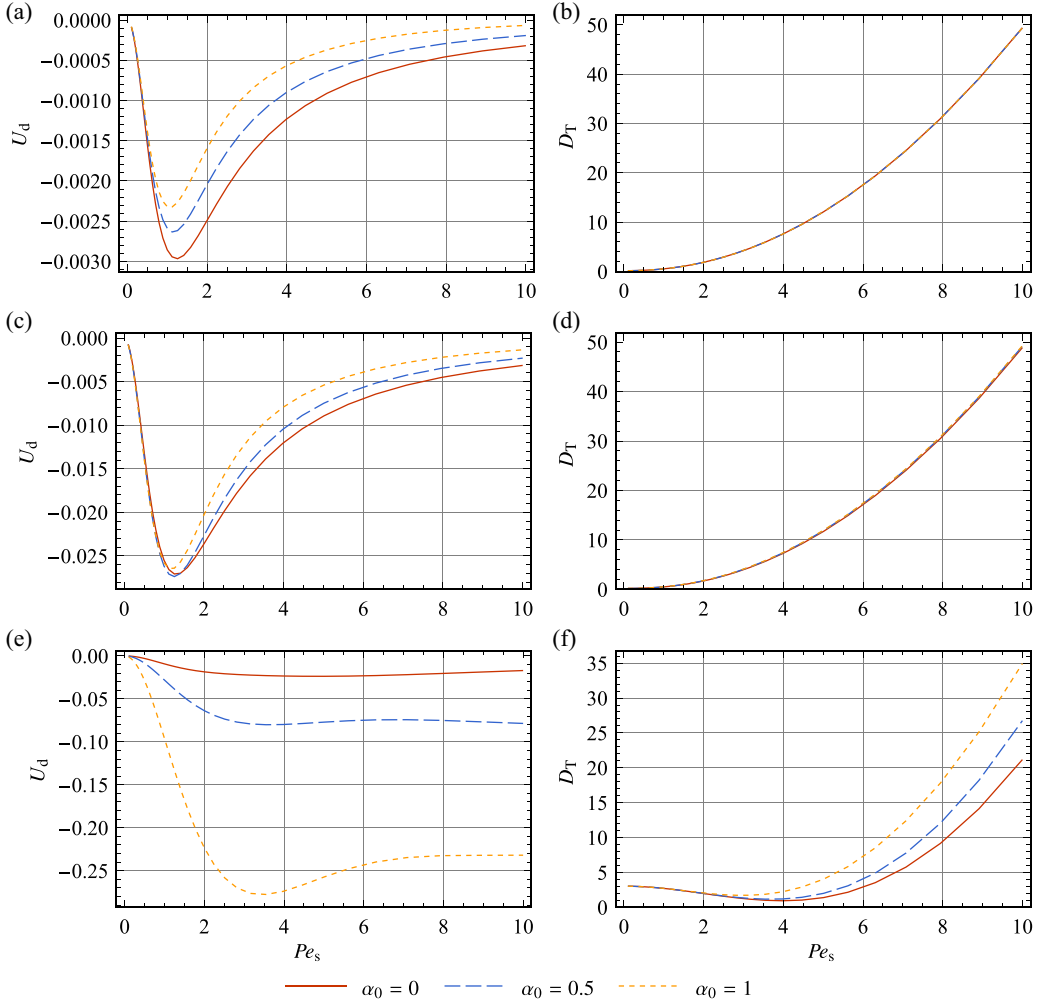


FIG. 7. Overall drift U_d and dispersivity D_T as functions of swimming Péclet number Pe_s under the reflective boundary conditions with fixed bias parameter $\lambda = 2$. Top, $Pe_f = 0.1$; middle, $Pe_f = 1$; bottom, $Pe_f = 10$. In all cases, $D_t = 1/6$.

Similarly, the dispersivity D_T can be also divided into two parts: the swimming-induced dispersivity and the advection-induced dispersivity. However, unlike the drift U_d , the dispersivity D_T shows nonmonotonic variation as a function of Pe_s only when the background flow is strong, i.e., $Pe_f = 10$. The monotonic variations in Figs. 6(b), 6(c) 7(b), and 7(c) are dominated by the swimming-induced dispersivity, which is positively correlated to the swimming ability Pe_s . In this swimming-dominated region, D_T shows negligible variation when we change Pe_f from 0.1 to 1, as shown in Figs. 6(b), 6(c) 7(b), and 7(c). However, the nonmonotonic variations of D_T in Figs. 6(f) and 7(f) illustrate the importance of the advection-induced dispersivity when Pe_f is large. As shown in Fig. 3, increasing Pe_s from 0.1 to 1 enhances the gravitactic focusing. When the background flow is strong, i.e., in the advection-dominated region, the enhanced gravitactic focusing leads to a decrease in advection-induced dispersivity and a decrease in overall dispersivity: the classical shear-enhanced (Taylor) dispersion is undermined. As the swimming Péclet number Pe_s continues increasing and the dispersivity is dominated by the swimming part, the overall dispersivity D_T again shows a positive correlation with Pe_s .

2. Influence of the bias parameter

As shown in Figs. 6(a), 6(c) and 6(e), U_d is negatively related to the bias parameter λ . As discussed in Sec. IV A 1, the gravitactic focusing is more intensive when λ is larger, and more microorganisms concentrate near the upper wall than in the bulk. The intensive gravitactic focusing results in a negative drift U_d to the mean flow. In Figs. 6(b), 6(d) and 6(f), the D_T - Pe_s curves of microorganisms with different bias parameters are almost the same. In other words, the bias parameter has little effect on the overall dispersivity but significantly affects the overall drift.

3. Influence of the shape factor

To characterize the influence of the shape anisotropy, we fix the bias parameter $\lambda = 2$ and change α_0 in $[0,1]$. The influence of the shape factor α_0 on U_d is rather complex. As discussed in Sec. IV A 2, a larger shape factor α_0 will enhance the accumulation at the walls. Thus slender microorganisms would have larger drift to the mean flow if we only consider the advection. However, in contrast to Fig. 7(e), slender microorganisms have a smaller drift to the mean flow in Figs. 7(a) and 7(c). This nonmonotonic behavior can be understood by considering the orientational distribution of microorganisms when the swimming effect is dominant, which is the situation in Figs. 7(a) and 7(c). When swimming is dominant, the drift is mainly contributed by $\langle P_0^\infty Pe_s \cos \theta \rangle$. We have realized that slender microorganisms have polarized orientational distribution with nearly equal likelihood of upstream swimming and downstream swimming. This polarized swimming behavior is the cause of smaller drift to the mean flow when the swimming is dominant. Instead, when the advection is dominant, slender microorganisms with more intensive accumulation at walls have a larger drift to the mean flow.

We now discuss the influence of shape anisotropy on the overall dispersivity. When Pe_f is not large, as shown in Figs. 7(b) and 7(d), microorganisms with different shape anisotropy show negligible difference regarding their dispersivity. It is evident that microorganisms with smaller α_0 have more uniform vertical distribution and subsequently larger advection-induced dispersivity. However, due to the shear alignment, microorganisms with larger α_0 have more polarized orientational distribution and hence have a larger swimming-induced dispersivity. The neutralization of these two effects leads to the indistinguishable overall dispersivity of microorganisms with different shape anisotropy. The situation is different when Pe_f is large: with a large Pe_f , the orientational distribution of elongated microorganisms is highly polarized, as shown in Fig. 5. Although the strength of shear-induced dispersion cannot be fully taken as it is taken by the spherical microorganisms, the polarized orientational distribution enables elongated ones to diffuse more rapidly.

C. Influence of wall accumulation

The Robin type boundary conditions have been used to account for the wall accumulation [27,44,45]; here we present an analysis of the effect of the wall accumulation on the dispersion process. We also keep $D_t = 1/6$ under the Robin type boundary conditions to avoid the singularity when $D_t \rightarrow 0$.

As shown in Fig. 8, under the Robin type boundary conditions, even the nongyrotactic spherical microorganisms have nonuniform distribution: concentration near the boundaries is higher than in the bulk. This is in contrast to the uniform distribution under the reflective boundary conditions. Instead of being balanced by the specular reflection flux under the reflective boundary conditions, the swimming flux is balanced by the diffusion, which requires higher concentration near the boundaries.

The influence of gyrotaxis intensity λ on the vertical distribution is similar to that under the reflective boundary conditions: increasing λ enhances gravitactic focusing. However, the swimming ability Pe_s has a different influence on the vertical distribution compared with the cases under the reflective boundary conditions. Larger Pe_s means a stronger swimming ability or equivalently stronger

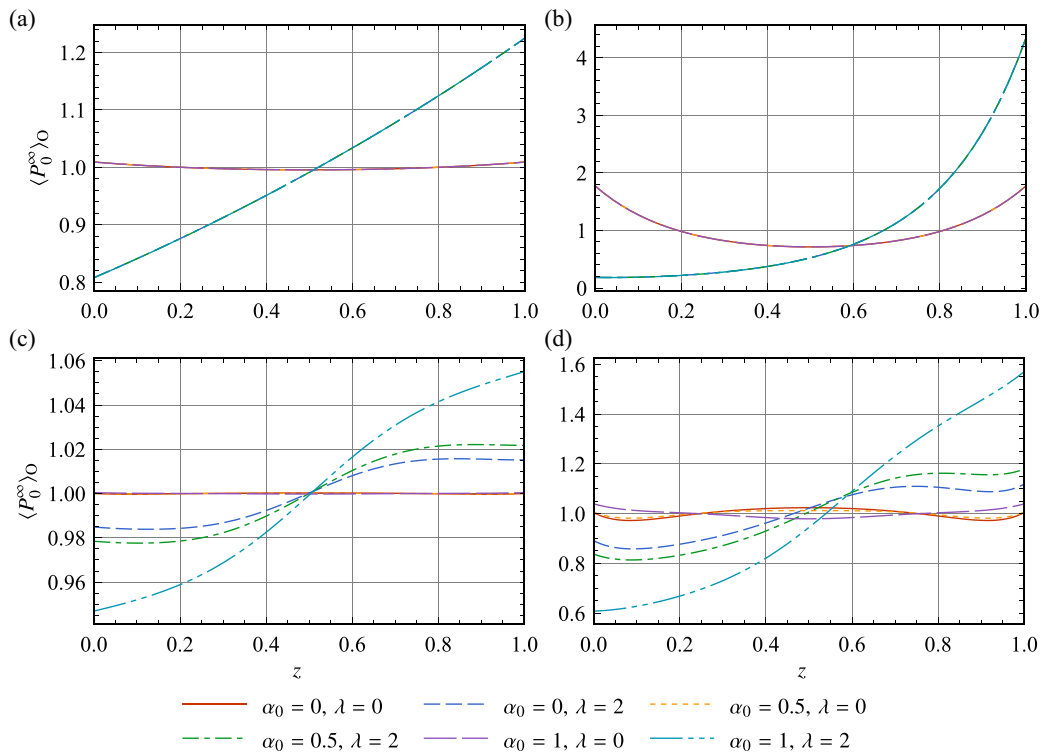


FIG. 8. Vertical distributions $\langle P_0^\infty \rangle_0$ of microorganisms under the Robin type boundary conditions. Pe_s at left and right are 0.1 and 1, respectively. Pe_f at top and bottom are 0.1 and 10, respectively. $D_t = 1/6$ in all cases.

confinement. Under the Robin boundary condition, the greater swimming-induced probability flux at the boundaries induces more intensive accumulation [56], which can be seen by comparing Figs. 8(a) and 8(b). In contrast, under the reflective boundary conditions, the microorganisms are reflected further and thus have no wall accumulation.

It can be seen clearly from Fig. 8 that the increased Pe_f leads to a decreased wall accumulation for nongyrotactic microorganisms and a decreased gravitactic focusing for gyrotactic ones. However, this variation is not obvious under the reflective boundary conditions, as shown in Fig. 4. This difference is due to the reduced wall accumulation; namely, as Pe_f increases, the rapid rotation of particles suppresses the wall-normal polarization and wall accumulation, as can be seen clearly in Fig. 9.

For the shape anisotropy α_0 , it enhances the accumulation at the upper wall, as shown in Fig. 8, but the enhancement is significant only when Pe_f is large, corresponding to a strong shear alignment effect.

The drift U_d and dispersivity D_T under the Robin boundary conditions are characterized as functions of the flow Péclet number Pe_f in Fig. 10. U_d of different microorganisms can be well understood by considering their vertical and orientational distribution. As shown before, shape anisotropy enhances accumulation near the walls, thus elongated microorganisms have larger drift to the mean flow. We can qualitatively account for the crossed lines in Figs. 10(a) and 10(c) considering the concentration variation as the flow is increased. In weak flows, gyrotaxis overwhelms shape-anisotropy-induced accumulation, thus gyrotactic microorganisms have larger drift to the mean flow. In strong flows, the situation is the opposite. Thus the most elongated nongyrotactic microorganisms ($\alpha_0 = 1, \lambda = 0$) have smaller drift to the mean flow at first and then larger.

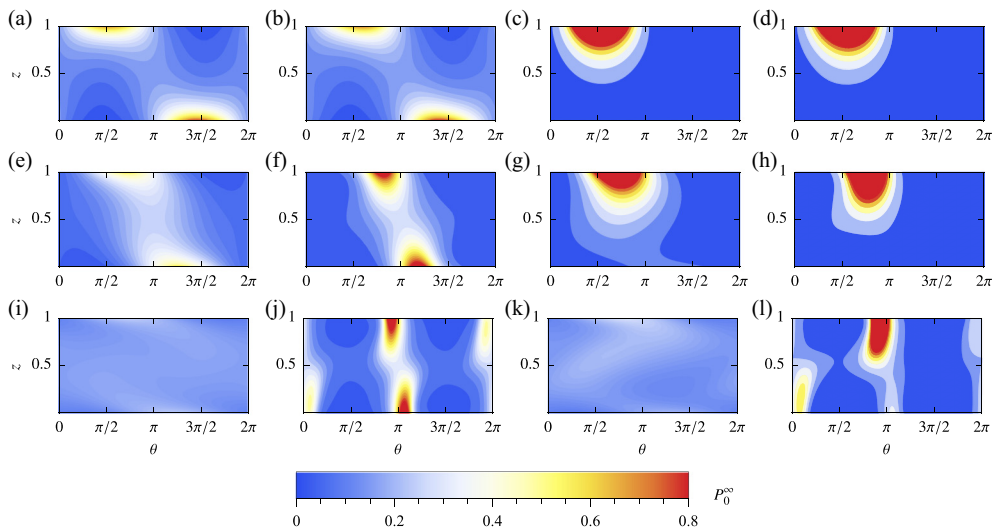


FIG. 9. $P_0^\infty(z, \theta)$ of microorganisms in the local space \mathbf{q} under the Robin type boundary conditions. First row, $Pe_f = 0.1$; second row, $Pe_f = 1$; third row, $Pe_f = 10$. The left two columns are for nongyrotactic microorganisms and the right two columns are for gyrotactic microorganisms with $\lambda = 2$. $\alpha = 0$ in the first column and third column and $\alpha = 1$ in the second column and fourth column. $Pe_s = 1$, $D_t = 1/6$ in all cases.

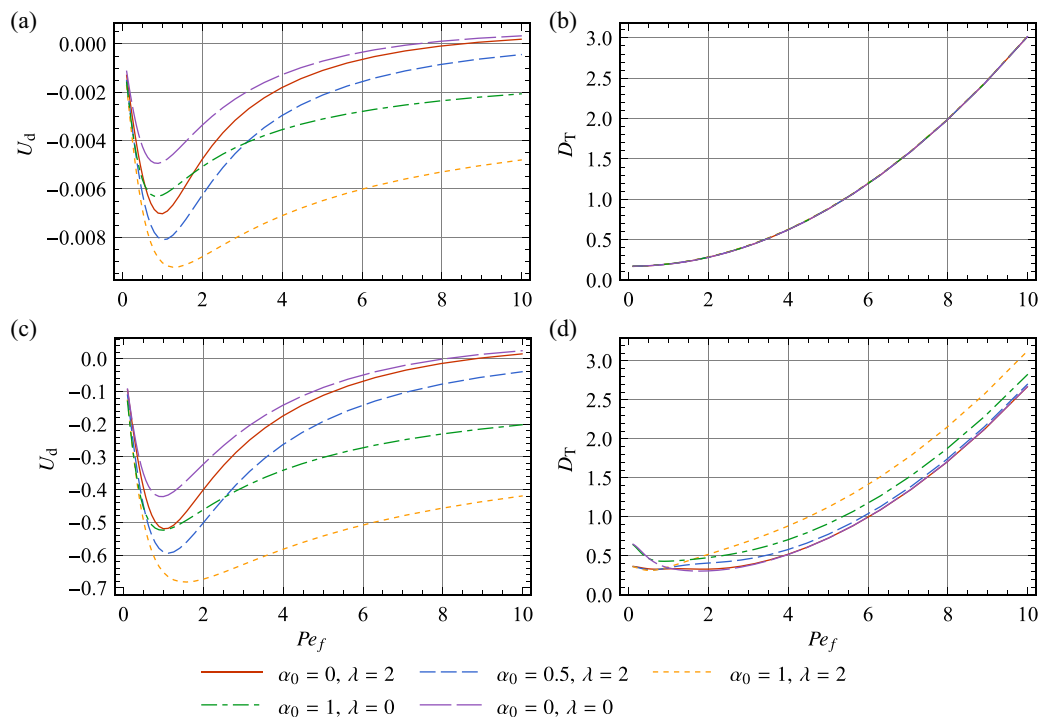


FIG. 10. Overall drift U_d and dispersivity D_T as functions of swimming Péclet number Pe_f under the Robin type boundary conditions. Top, $Pe_s = 0.1$; bottom, $Pe_s = 1$. $D_t = 1/6$ in all cases.

The nonmonotonic variations of U_d as a function of Pe_f can be understood by considering two different influential effects. First, we neglect to consider the variation of concentration when Pe_f increases, because more microorganisms are distributed in the near-boundary regions than in the bulk for both gyrotactic and nongyrotactic types, thus U_d decreases. Second, we consider the variation of concentration alone; as shown in Fig. 8, concentration in the bulk of both gyrotactic and nongyrotactic microorganisms increases as Pe_f increases, which increases U_d . With the analysis above, the nonmonotonic variations of U_d as a function of Pe_f can be understood.

Additionally, upstream swimming (negative drift) and the transition to downstream swimming of nongyrotactic microorganisms are studied by several researchers [27,40,45,57,58]. Specifically, we note that the upstream swimming in our paper is in the flow-fixed frame, which may contain the upstream swimming in the laboratory-fixed frame at very small Pe_f . A detailed analysis of upstream swimming of active particles can be seen in the paper of Peng and Brady [27], where the Robin type boundary conditions are also imposed.

The dispersivity D_T is nearly monotonic as a function of Pe_f . For the situation depicted in Fig. 10(b), advection-induced dispersivity is dominant because of negligible swimming-induced dispersivity ($Pe_s = 0.1$). In this situation, the differences between the vertical distributions of different microorganisms, as depicted in Fig. 8(c), are small in magnitude compared to the differences depicted in Fig. 8(d), which explains the negligible differences of overall dispersivity. However, as Pe_s gets larger, the differences between vertical distributions of microorganisms become more significant, i.e., differences between advection-induced dispersivity become more significant. In the meantime, swimming-induced dispersivity characterized by the orientational distribution also becomes influential. These two effects lead to the crossed and nonmonotonic lines in Fig. 10(d).

V. CONCLUSIONS

This paper extends the one-step GTD theory to the active dispersion process of gyrotactic microorganisms in a horizontal plane Poiseuille flow. With two sets of basis functions satisfying the reflective and the Robin type boundary conditions, respectively, the local distribution, vertical distribution, drift, and dispersivity are obtained by the corresponding series expansion.

This paper has analyzed the influence of the gravitactic focusing and the wall accumulation on the dispersion process. A detailed analysis regarding the bias parameter, swimming Péclet number, shape factor, and velocity of ambient flow is carried out. The gravitactic focusing is first analyzed alone by imposing the reflective boundary conditions which exclude the near-boundary accumulation effect. Second, to account for the near-boundary accumulation effect, the Robin type boundary conditions are also considered. The major difference between the reflective boundary conditions and the Robin type boundary conditions, i.e., the difference between considering gravitactic focusing alone and considering both accumulation effects, is the influences of swimming ability. In the absence of translational diffusivity, i.e., $D_t = 0$, the asymptotic exponential distribution of Beaton *et al.* [17] is consistent with our results: the gravitactic focusing is enhanced by decreasing the swimming ability (decreasing stone skipping). When a constant translational diffusivity is applied, the gravitactic focusing shows nonmonotonic variation as the swimming ability increases: when the swimming ability is weak, the intensive gravitactic focusing is weakened by translational diffusion; when the swimming ability is strong, the stone skipping also inhibits gravitactic focusing; only in a moderate range of swimming ability does gravitactic focusing reach its maximum. In contrast, under the Robin type boundary conditions, the accumulation at the upper wall is enhanced when swimming ability increases because of the wall accumulation mechanism. A larger bias parameter induces more intensive gravitactic focusing at the upper wall. Slender gyrotactic microorganisms are subject to the shear alignment effect, which polarizes the orientational distribution and induces greater concentration at the upper wall.

The drift is the weighted average of the local flow speed plus longitudinal swimming speed. In a Poiseuille flow, either the wall accumulation or the gravitactic focusing leads to a negative drift to the mean flow. Generally speaking, the more intensive the accumulation at walls is, the larger

the drift to the mean flow is. Therefore, the drift can be enhanced by increasing the bias parameter and the shape factor. Notably, due to the change in the local space distribution, a transition between upstream swimming and downstream swimming of nongyrotactic microorganisms can be found in a moderate range of Pe_f . We note that this upstream swimming is in the flow-fixed frame, which may contain the upstream swimming in the laboratory-fixed frame.

The dispersivity should be analyzed in conjunction with the relative strength of swimming-induced dispersivity and advection-induced dispersivity. The swimming-induced dispersivity and the advection-induced dispersivity are highly coupled with the shape factor, flow Péclet number, and swimming Péclet number, leading to nonmonotonic variations of the total effective dispersivity.

This paper provides results for the dispersion process of gyrotactic microorganisms in a horizontal Poiseuille flow. However, this paper only focuses on the long-time asymptotic state; the evolution process containing anomalous diffusion regimes is not considered. The idealized reflective boundary conditions are only mathematically meaningful for microorganisms. The Robin type boundary conditions, although they can partially explain some phenomena, did not consider the complex behaviors of microorganisms at walls [59] and do not hold for the zero translational diffusivity limit $D_t = 0$. For microorganisms transport in flows with free surfaces, which is also of great importance to practical applications like thin phytoplankton layers [60], the boundary conditions are more complex due to the diverse dynamics at different surfaces [61–63]. Further work can be done in the research of boundary conditions at both the individual level and the continuum level.

ACKNOWLEDGMENTS

This work is supported by the National Natural Science Foundation of China (Grants No. 51879002 and No. 52079001).

APPENDIX A: COMPARISON WITH INDIVIDUAL-BASED METHOD

We compare our solution with individual-based method (IBM). The dimensionless governing equations for the position and orientation of a swimmer are discretized in a forward Euler scheme:

$$\begin{aligned} \Delta x &= Pe_f U \Delta t + Pe_s \cos \theta \Delta t + \Delta x^B, \\ \Delta z &= Pe_s \sin \theta \Delta t + \Delta z^B, \\ \Delta \theta &= \left(-\frac{1}{2} Pe_f \frac{\partial U}{\partial z} + \frac{1}{2} \alpha_0 Pe_f \frac{\partial U}{\partial z} \cos 2\theta + \lambda \cos \theta \right) \Delta t + \Delta \theta^B, \end{aligned} \quad (\text{A1})$$

where Δt is the time step. Δx^B and $\Delta z^B \sim \mathcal{N}(0, 2D_t \Delta t)$ and $\Delta \theta^B \sim \mathcal{N}(0, 2\Delta t)$. Let (x_n, z_n, θ_n) denote the n th step coordinates of a swimmer; the reflective boundary conditions implemented in IBM are

$$\begin{aligned} z_n &\rightarrow 2 - z_n, & \theta_n &\rightarrow -\theta_n, & \text{if } z_n > 1, \\ z_n &\rightarrow -z_n, & \theta_n &\rightarrow -\theta_n, & \text{if } z_n < 0, \end{aligned} \quad (\text{A2})$$

where \rightarrow denotes assignment. For the Robin type boundary conditions, the corresponding treatment in IBM is

$$\begin{aligned} z_n &\rightarrow 1, & \theta_n &\rightarrow \theta_n, & \text{if } z_n > 1, \\ z_n &\rightarrow 0, & \theta_n &\rightarrow \theta_n, & \text{if } z_n < 0, \end{aligned} \quad (\text{A3})$$

which is the potential-free algorithm [64]. We use 10^5 particles and a time step $\Delta t = 10^{-4}$ to ensure good data. The particles are initially located at $z = 1/2$ with their orientations θ uniformly distributed in $[0, 2\pi)$. As shown in Figs. 11–13, the results of GTD and the results of IBM are in good agreement.

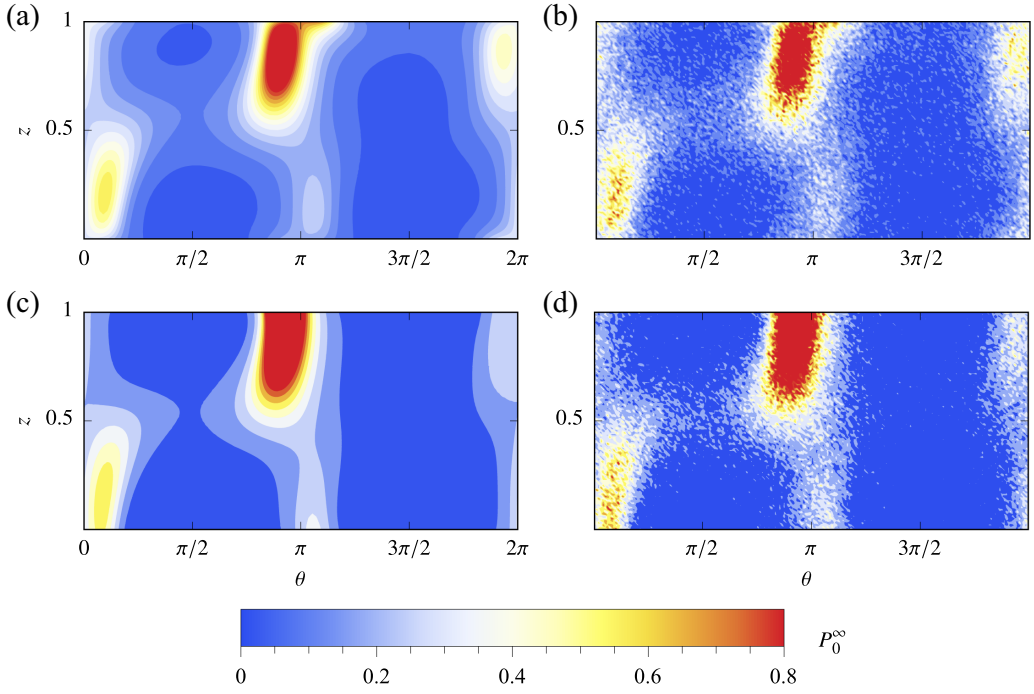


FIG. 11. $P_0^\infty(z, \theta)$ of microorganisms in the local space \mathbf{q} . First row: Reflective boundary conditions. Second row: Robin type boundary conditions. Left column: Results of GTD. Right column: Results of IBM. In all cases, $Pe_s = 1$, $Pe_f = 10$, $\alpha_0 = 1$, $\lambda = 2$, $D_t = 1/6$.

APPENDIX B: BASIS FUNCTION

To perform the series expansion, we seek the basis functions satisfying the reflective boundary conditions, and then we obtain the solution with the Galerkin method. For the eigenfunctions of the operator

$$\mathcal{M} = \frac{\partial^2}{\partial z^2} + \frac{\partial^2}{\partial \theta^2} \quad (\text{B1})$$

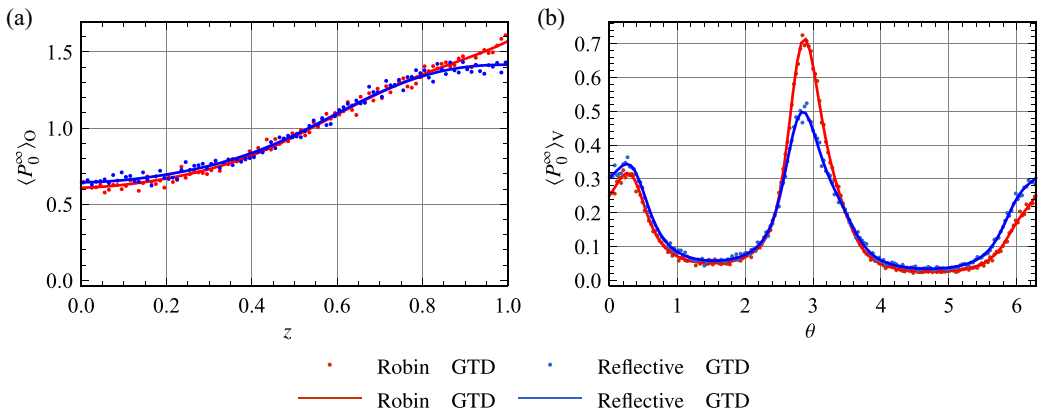
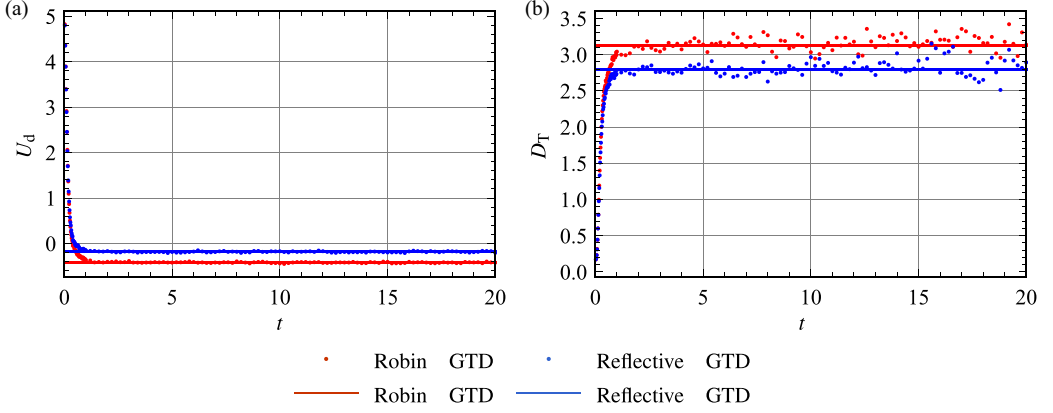


FIG. 12. Vertical distribution $\langle P_0^\infty \rangle_O$ and orientational distribution $\langle P_0^\infty \rangle_V$ of microorganisms under different boundary conditions. In all cases, $Pe_s = 1$, $Pe_f = 10$, $\alpha_0 = 1$, $\lambda = 2$, $D_t = 1/6$.


 FIG. 13. Evolution and steady state of drift U_d and dispersivity D_T .

on the local space that satisfy the reflective boundary conditions, bounded and periodic conditions can be used as the basis functions. The inner product of given functions f and g is

$$(f, g) \triangleq \int_0^1 dz \int_0^{2\pi} f(z, \theta) g(z, \theta) d\theta. \quad (\text{B2})$$

\mathcal{M} is a self-adjoint operator under the conditions (18)–(20).

The eigenfunctions for \mathcal{M} are

$$\begin{aligned} & A_r \cos(n\pi z), \\ & B_r \cos(n\pi z) \cos(m\theta), \\ & B_r \sin(n\pi z) \sin(m\theta), \end{aligned} \quad (\text{B3})$$

where $m = 1, 2, \dots, n = 0, 1, 2, \dots$, and

$$A_r = \begin{cases} \sqrt{\frac{1}{2\pi}}, & n = 0, \\ \sqrt{\frac{1}{\pi}}, & n \neq 0. \end{cases} \quad (\text{B4})$$

$$B_r = \begin{cases} \sqrt{\frac{1}{\pi}}, & n = 0, \\ \sqrt{\frac{2}{\pi}}, & n \neq 0. \end{cases} \quad (\text{B5})$$

The reflective basis given in (B3) is orthogonal and normalized; then P_0^∞ can be expanded into

$$P_0^\infty(z, \theta) = \sum_{i=1}^{\infty} q_i e_i^r(z, \theta), \quad (\text{B6})$$

where e_i^r are the functions given in reflective basis, and q_i are coefficients to be determined by a Galerkin method. In our calculation, the series expansion is truncated up to $n = m = 20$, which can capture the gravitactic focusing in the vertical direction.

Similarly, for the eigenfunctions of operator \mathcal{M} on the local space that satisfy the Robin type boundary conditions, bounded and periodic conditions can be used as the basis functions for G_0 . The eigenfunctions under the Robin type boundary conditions are

$$\begin{aligned} & A_R \cos(n\pi z), \\ & B_R \cos(n\pi z) \cos(m\theta), \\ & B_R \cos(n\pi z) \sin(m\theta), \end{aligned} \quad (\text{B7})$$

where $m = 1, 2, \dots, n = 0, 1, 2, \dots$, and

$$A_R = \begin{cases} \sqrt{\frac{1}{2\pi}}, & n = 0, \\ \sqrt{\frac{1}{\pi}}, & n \neq 0. \end{cases} \quad (\text{B8})$$

$$B_R = \begin{cases} \sqrt{\frac{1}{\pi}}, & n = 0, \\ \sqrt{\frac{2}{\pi}}, & n \neq 0. \end{cases} \quad (\text{B9})$$

-
- [1] W. M. Durham, J. O. Kessler, and R. Stocker, Disruption of vertical motility by shear triggers formation of thin phytoplankton layers, *Science* **323**, 1067 (2009).
- [2] O. A. Croze, G. Sardina, M. Ahmed, M. A. Bees, and L. Brandt, Dispersion of swimming algae in laminar and turbulent channel flows: Consequences for photobioreactors, *J. R. Soc. Interface* **10**, 20121041 (2013).
- [3] J. O. Kessler, Hydrodynamic focusing of motile algal cells, *Nature (London)* **313**, 218 (1985).
- [4] M. A. Bees and O. A. Croze, Dispersion of biased swimming micro-organisms in a fluid flowing through a tube, *Proc. R. Soc. A* **466**, 2057 (2010).
- [5] A. Dehkharghani, N. Waisbord, J. Dunkel, and J. S. Guasto, Bacterial scattering in microfluidic crystal flows reveals giant active Taylor-Aris dispersion, *Proc. Natl. Acad. Sci. USA* **116**, 11119 (2019).
- [6] Rothschild, Non-random distribution of bull spermatozoa in a drop of sperm suspension, *Nature (London)* **198**, 1221 (1963).
- [7] A. P. Berke, L. Turner, H. C. Berg, and E. Lauga, Hydrodynamic attraction of swimming microorganisms by surfaces, *Phys. Rev. Lett.* **101**, 038102 (2008).
- [8] R. Rusconi, J. S. Guasto, and R. Stocker, Bacterial transport suppressed by fluid shear, *Nat. Phys.* **10**, 212 (2014).
- [9] C. Bechinger, R. Di Leonardo, H. Löwen, C. Reichhardt, G. Volpe, and G. Volpe, Active particles in complex and crowded environments, *Rev. Mod. Phys.* **88**, 045006 (2016).
- [10] J. Arrieta, M. Polin, R. Saleta-Piersanti, and I. Tuval, Light control of localized photobioconvection, *Phys. Rev. Lett.* **123**, 158101 (2019).
- [11] R. Rusconi and R. Stocker, Microbes in flow, *Curr. Opin. Microbiol.* **25**, 1 (2015).
- [12] A. J. T. M. Mathijssen, T. N. Shendruk, J. M. Yeomans, and A. Doostmohammadi, Upstream swimming in microbiological flows, *Phys. Rev. Lett.* **116**, 028104 (2016).
- [13] T. J. Pedley and J. O. Kessler, Hydrodynamic phenomena in suspensions of swimming microorganisms, *Annu. Rev. Fluid Mech.* **24**, 313 (1992).
- [14] R. N. Bearon, M. A. Bees, and O. A. Croze, Biased swimming cells do not disperse in pipes as tracers: A population model based on microscale behaviour, *Phys. Fluids* **24**, 121902 (2012).
- [15] M. Cencini, G. Boffetta, M. Borgnino, and F. De Lillo, Gyrotactic phytoplankton in laminar and turbulent flows: A dynamical systems approach, *Eur. Phys. J. E* **42**, 31 (2019).
- [16] S. Ghorai, Gyrotactic trapping: A numerical study, *Phys. Fluids* **28**, 041901 (2016).
- [17] R. N. Bearon, A. L. Hazel, and G. J. Thorn, The spatial distribution of gyrotactic swimming micro-organisms in laminar flow fields, *J. Fluid Mech.* **680**, 602 (2011).
- [18] A. M. Roberts, Mechanisms of gravitaxis in *Chlamydomonas*, *Biol. Bull* **210**, 78 (2006).
- [19] J. P. Hernandez-Ortiz, C. G. Stoltz, and M. D. Graham, Transport and collective dynamics in suspensions of confined swimming particles, *Phys. Rev. Lett.* **95**, 204501 (2005).
- [20] G. Li and J. X. Tang, Accumulation of microswimmers near a surface mediated by collision and rotational Brownian motion, *Phys. Rev. Lett.* **103**, 078101 (2009).
- [21] G. Taylor, Dispersion of soluble matter in solvent flowing slowly through a tube, *Proc. R. Soc. A* **219**, 186 (1953).
- [22] G. Taylor, The dispersion of matter in turbulent flow through a pipe, *Proc. R. Soc. A* **223**, 446 (1954).
- [23] R. Aris, On the dispersion of a solute in a fluid flowing through a tube, *Proc. R. Soc. A* **235**, 67 (1956).

- [24] R. Aris, On the dispersion of a solute by diffusion, convection and exchange between phases, *Proc. R. Soc. A* **252**, 538 (1959).
- [25] I. Frankel and H. Brenner, On the foundations of generalized Taylor dispersion theory, *J. Fluid Mech.* **204**, 97 (1989).
- [26] N. A. Hill and M. A. Bees, Taylor dispersion of gyrotactic swimming micro-organisms in a linear flow, *Phys. Fluids* **14**, 2598 (2002).
- [27] Z. Peng and J. F. Brady, Upstream swimming and Taylor dispersion of active Brownian particles, *Phys. Rev. Fluids* **5**, 073102 (2020).
- [28] T. J. Pedley and J. O. Kessler, A new continuum model for suspensions of gyrotactic micro-organisms, *J. Fluid Mech.* **212**, 155 (1990).
- [29] Y. Hwang and T. J. Pedley, Bioconvection under uniform shear: Linear stability analysis, *J. Fluid Mech.* **738**, 522 (2014).
- [30] Y. Hwang and T. J. Pedley, Stability of downflowing gyrotactic microorganism suspensions in a two-dimensional vertical channel, *J. Fluid Mech.* **749**, 750 (2014).
- [31] T. J. Pedley, Gyrotaxis in uniform vorticity, *J. Fluid Mech.* **762**, R6 (2015).
- [32] L. Zeng and T. J. Pedley, Distribution of gyrotactic micro-organisms in complex three-dimensional flows. Part 1. Horizontal shear flow past a vertical circular cylinder, *J. Fluid Mech.* **852**, 358 (2018).
- [33] O. A. Croze, R. N. Bearon, and M. A. Bees, Gyrotactic swimmer dispersion in pipe flow: Testing the theory, *J. Fluid Mech.* **816**, 481 (2017).
- [34] W. Jiang and G. Chen, Dispersion of active particles in confined unidirectional flows, *J. Fluid Mech.* **877**, 1 (2019).
- [35] H. Brenner and D. A. Edwards, *Macrotransport Processes* (Butterworth-Heinemann, Stoneham, MA, 1993).
- [36] W. Jiang and G. Chen, Dispersion of gyrotactic micro-organisms in pipe flows, *J. Fluid Mech.* **889**, A18 (2020).
- [37] T. Ishikawa, Vertical dispersion of model microorganisms in horizontal shear flow, *J. Fluid Mech.* **705**, 98 (2012).
- [38] S. Maretvadakethope, E. E. Keaveny, and Y. Hwang, The instability of gyrotactically trapped cell layers, *J. Fluid Mech.* **868**, R5 (2019).
- [39] E. Lauga, W. R. DiLuzio, G. M. Whitesides, and H. A. Stone, Swimming in circles: Motion of bacteria near solid boundaries, *Biophys. J.* **90**, 400 (2006).
- [40] T. Kaya and H. Koser, Characterization of hydrodynamic surface interactions of *Escherichiacoli* cell bodies in shear flow, *Phys. Rev. Lett.* **103**, 138103 (2009).
- [41] J. P. Hernandez-Ortiz, P. T. Underhill, and M. D. Graham, Dynamics of confined suspensions of swimming particles, *J. Phys.: Condens. Matter* **21**, 204107 (2009).
- [42] G. Li, J. Besson, L. Nisimova, D. Munger, P. Mahautmr, J. X. Tang, M. R. Maxey, and Y. V. Brun, Accumulation of swimming bacteria near a solid surface, *Phys. Rev. E* **84**, 041932 (2011).
- [43] K. Drescher, J. Dunkel, L. H. Cisneros, S. Ganguly, and R. E. Goldstein, Fluid dynamics and noise in bacterial cell–cell and cell–surface scattering, *Proc. Natl. Acad. Sci. USA* **108**, 10940 (2011).
- [44] J. Elgeti and G. Gompper, Wall accumulation of self-propelled spheres, *Europhys. Lett.* **101**, 48003 (2013).
- [45] B. Ezhilan and D. Saintillan, Transport of a dilute active suspension in pressure-driven channel flow, *J. Fluid Mech.* **777**, 482 (2015).
- [46] B. Ezhilan, A. A. Pahlavan, and D. Saintillan, Chaotic dynamics and oxygen transport in thin films of aerotactic bacteria, *Phys. Fluids* **24**, 091701 (2012).
- [47] G. Volpe, S. Gigan, and G. Volpe, Simulation of the active Brownian motion of a microswimmer, *Am. J. Phys.* **82**, 659 (2014).
- [48] A. Bricard, J.-B. Caussin, D. Das, C. Savoie, V. Chikkadi, K. Shitara, O. Chepizhko, F. Peruani, D. Saintillan, and D. Bartolo, Emergent vortices in populations of colloidal rollers, *Nat. Commun.* **6**, 7470 (2015).
- [49] M. Doi and S. F. Edwards, *The Theory of Polymer Dynamics* (Oxford University, Oxford, 1988), Vol. 75.

- [50] T. J. Pedley and J. O. Kessler, The orientation of spheroidal microorganisms swimming in a flow field, *Proc. R. Soc. B* **231**, 47 (1987).
- [51] F. P. Bretherton, The motion of rigid particles in a shear flow at low Reynolds number, *J. Fluid Mech.* **14**, 284 (1962).
- [52] J. O. Kessler, Individual and collective fluid dynamics of swimming cells, *J. Fluid Mech.* **173**, 191 (1986).
- [53] Y. Zeng and B. Liu, Self-propelling and rolling of a sessile-motile aggregate of the bacterium *Caulobacter crescentus*, *Commun. Biol.* **3**, 587 (2020).
- [54] K. Drescher, K. C. Leptos, I. Tuval, T. Ishikawa, T. J. Pedley, and R. E. Goldstein, Dancing *volvox*: Hydrodynamic bound states of swimming algae, *Phys. Rev. Lett.* **102**, 168101 (2009).
- [55] X. Chen, Y. Wu, and L. Zeng, Migration of gyrotactic micro-organisms in water, *Water* **10**, 1455 (2018).
- [56] H. Nili, M. Kheyri, J. Abazari, A. Fahimniya, and A. Najj, Population splitting of rodlike swimmers in Couette flow, *Soft Matter* **13**, 4494 (2017).
- [57] J. Hill, O. Kalkanci, J. L. McMurry, and H. Koser, Hydrodynamic surface interactions enable *Escherichia coli* to seek efficient routes to swim upstream, *Phys. Rev. Lett.* **98**, 068101 (2007).
- [58] T. Kaya and H. Koser, Direct upstream motility in *Escherichia coli*, *Biophys. J.* **102**, 1514 (2012).
- [59] V. Kantsler, J. Dunkel, M. Polin, and R. E. Goldstein, Ciliary contact interactions dominate surface scattering of swimming eukaryotes, *Proc. Natl. Acad. Sci. USA* **110**, 1187 (2013).
- [60] W. M. Durham and R. Stocker, Thin phytoplankton layers: Characteristics, mechanisms, and consequences, *Annu. Rev. Mater. Sci.* **4**, 177 (2012).
- [61] R. Di Leonardo, D. Dell'Arciprete, L. Angelani, and V. Iebba, Swimming with an image, *Phys. Rev. Lett.* **106**, 038101 (2011).
- [62] D. Lopez and E. Lauga, Dynamics of swimming bacteria at complex interfaces, *Phys. Fluids* **26**, 071902 (2014).
- [63] S. Bianchi, F. Saglimbeni, G. Frangipane, D. Dell'Arciprete, and R. D. Leonardo, 3D dynamics of bacteria wall entrapment at a water-air interface, *Soft Matter* **15**, 3397 (2019).
- [64] D. M. Heyes and J. R. Melrose, Brownian dynamics simulations of model hard-sphere suspensions, *J. Non-Newtonian Fluid Mech.* **46**, 1 (1993).